SUPPLEMENTAL INFORMATION

LC-MS/MS suggests that hole hopping in cytochrome c peroxidase protects its heme from oxidative modification by excess H_2O_2

Meena Kathiresan and Ann M. English*

Contents

Fig. S1: Tryptic peptides T1-T34 predicted for Ccp1 2
LC-MS and LC-MS/MS analyses 3
Table S1: Oxidative modifications considered in database searching 4
Table S2: Peak areas (*PA*s) of the internal reference peptides in the Ccp1 tryptic digests 5
Table S3: Monoisotopic *m/z* values of the MH^+ ions of tryptic peptides observed in the digests of H_2O_2-oxidzed Ccp1 6
Table S4: CCP activity of H_2O_2-oxidized Ccp1 8
Table S5. Peptides T21 (M172, H175) and T14+T15 (W126, C128) are oxidized at two residues 9
Table S6: Assignment of sequence ions in the MS/MS spectrum of the T6 native peptide 10
Table S7: Assignment of sequence ions in the MS/MS spectrum of the T6 oxidized peptide 11
Fig. S2: Characterization of *intramolecular* dityrosine crosslinks in H_2O_2-oxidized Ccp1 12
Fig. S3. LC-MS/MS analysis of dityrosine formation in tryptic peptides T8 and T26 13
Fig. S4: LC-MS analysis of hemin released from Ccp1 exposed to 0, 10 and 100 M eq of H_2O_2 14
Fig. S5: LC-MS/MS analysis of H175 and H52 oxidation in tryptic peptides T21 and T7 15
Standard MD simulations of Ccp1 in water with O_2 molecules 16
Fig. S6: MD simulation of Ccp1 in water with 100 added O_2 molecules 17
Fig. S7: Ultraviolet circular dichroism spectrum of Ccp1 oxidized with 0, 1 and 10 M eq of H_2O_2 18
Table S8: O_2 and water exposure of the oxidizable residues in Ccp1 19
Scheme S1: Proposed pathway of tryptophan oxidation 20
Scheme S2: Proposed pathway of tyrosine oxidation 20
Scheme S3: Proposed pathway of histidine oxidation 21
Scheme S4: Proposed pathway of cysteine oxidation 21
Scheme S5: Proposed pathway of methionine oxidation 22
Supplemental literature cited 22

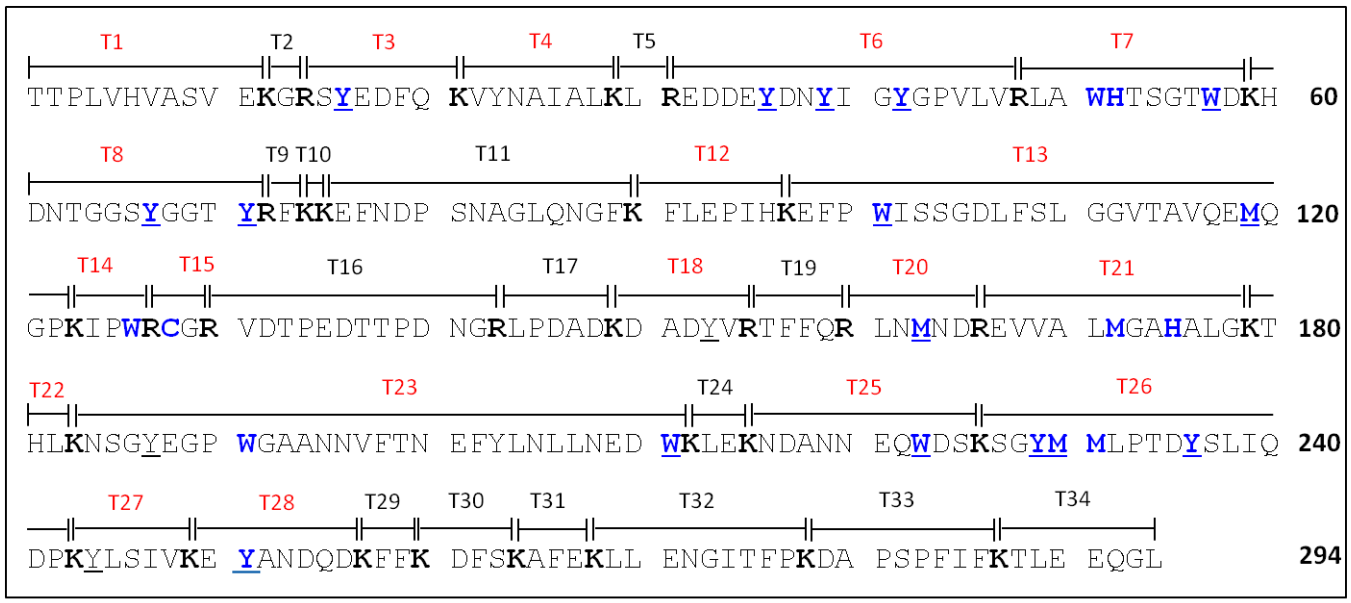

Fig. S1: Tryptic peptides T1-T34 predicted for Ccp1

The protein's sequence is divided in blocks of 10 residues and the trypsin cleavage sites arginine (**R**) and lysine (**K**) residues are bolded. Peptides that contain oxidizable residues (M, C, Y, W, H) are labeled in **red font** and the 24 residues found to be > 5% oxidized are in **blue font**. Solvent-exposed oxidizable residues are underlined.

LC-MS and LC-MS/MS analyses

LC-MS analysis of intact apo- and holoCcp1 ± H_2O_2 and of Ccp1-derived heme. Solutions of oxidized apo- and holoCcp1 were diluted into 5% aqueous acetonitrile/0.1% formic acid (MS solvent) and 2 µL aliquots were loaded onto a reversed-phase Zorbax 300SB-CN (2.1 x 150 mm, 5 µm) column attached to an Agilent 1200 HPLC and equilibrated with the MS solvent at room temperature. Samples were eluted from the HPLC column at a flow rate of 0.2 mL/min with a 5-95% acetonitrile gradient over 5 min into the Z-Spray source of a QToF3 mass spectrometer (Waters). The acetonitrile concentration was held constant at 95% for 3 min, lowered to 5% over the next 3 min and the column was re-equilibrated with the MS solvent for 8 min prior to the next injection. Mass measurements were performed using the following QToF3 parameters: capillary voltage 3.5 kV, cone voltage 35 V, RF lens 50 V, source temperature 80°C and desolvation temperature 300 °C. Protein envelopes were deconvolved (MaxEnt1 algorithm, Waters) to give intact protein masses.

To monitor its integrity, the exact mass of the heme released at low pH from oxidized Ccp1 was recorded. The oxidized protein in the MS solvent was injected onto a reversed-phase C4 capillary column (100 µm x 4.0 cm) prepared in-house and attached to a NanoLC (EASY-nLC, Thermo Scientific). The column was equilibrated with the same solvent and samples were eluted at 200 nL/min with a 5-95% acetonitrile gradient into the nanoESI source of a LTQ Orbitrap Velos mass spectrometer (Thermo Scientific) and analyzed in full-scan mode (*m/z* 100–2000) in the Orbitrap high resolution mass analyzer (R=60,000 at *m/z* 400). Other instrument parameters were: electrospray voltage 3 kV, CID collision energy 35 V and heated capillary temperature 200 °C.

LC-MS/MS analysis of tryptic digests of oxidized Ccp1. Donor residues were identified by sequencing of the oxidized tryptic peptides. Untreated Ccp1 and oxidized Ccp1 were alkylated with 55 mM iodoacetamide for 30 min at room temperature and digested overnight with 12.5 ng/µL (1:20) of trypsin in 50 mM ammonium bicarbonate (pH 8.0)/100 µM DTPA at 37 °C. The digests were desalted on C18 Zip Tips and the tryptic peptides (5 µL/injection) were separated on a homemade reversed-phase C18 capillary column (100 µm x 6.5 cm) equilibrated with 2% aqueous acetonitrile/0.1% formic acid and attached to the NanoLC. Peptides were eluted at a flow rate of 200 nL/min into the nanoESI source of the Orbitrap mass spectrometer using a 2-94% acetonitrile gradient and analyzed in the Orbitrap as described for heme above. Sequence coverage from the peptide maps was routinely 96-100%, and included all the oxidizable residues shown in Fig. 1.

Precursor peptide ions were selected in MS1 using a mass exclusion threshold of 10 ppm and fragmented in the Velos linear ion trap at a collision energy of 35 V. MS2 fragments with an intensity count of ≥20 were analyzed with a mass tolerance of 0.8 u using Proteome Discoverer 1.3.0 software (Thermo Scientific) and the Sequest search engine with mass filters for the oxidative modifications listed in Table S1 in addition to cysteine alkylation by iodoacetamide (+ 57 u). Dynamic exclusion was enabled with a repeat count of 1, a repeat duration of 30 s and an excluded list size of 500. Sequest correlates the MS2 spectra with peptide sequences in the Ccp1 Fasta file downloaded from the NCBI website (ftp://ftp.ncbi.nlm.nih.gov/). Sequest's filters, XCorr (>2) and False Discovery Rate (<0.01), were implemented for confident peptide identification.

Table S1: Oxidative modifications considered in database searching [a]

Modification: candidate amino acids [b]	Δm (u) [c]
Monoxidation (ox): K, R, C, M, Y, H, P, W, F, D, N Dioxidation (diox): K, R, C, M, Y, H, P, W, F Trioxidation (triox): C	15.9949 31.9898 47.9847
Carbonylation: R, E, Q, I, L, K, V, W	13.9793
Hydroxykynurenine: W	19.9898
Kynurenine (kyn): W	3.9949
Pyrrolidinone: P	30.0105
Pyroglutamic acid: P	13.9792
Aspargine: H	23.0159
Aspartic acid: H	22.0319
Aspartylurea: H	10.0320
Formylaspargine: H	4.9790
Aspartate semialdehyde: M	32.0085
Homocysteic acid: M	33.9691
Dehydro (deH): K, R, C, M, Y, H, P, W, F, D, N [d]	1.00783

[a] Mass filters for these oxidative modifications were used with the Sequest search engine

[b] Reported products of single amino acid oxidation.[1,2]

[c] Difference in the monoisotopic mass of the oxidized and native form of the indicated amino acid.

[d] Crosslinked residues undergo loss of a hydrogen atom (see main text).

Table S2: Peak areas (*PA*s) of the internal reference peptides in the Ccp1 tryptic digests [a]

Peptide sequence	Obs MH^+ (*m/z*)	ppm error [b]	*PA* [c]			
			0:1 $[H_2O_2]$:[Ccp1]	**1:1 $[H_2O_2]$:[Ccp1]**	**5:1 $[H_2O_2]$:[Ccp1]**	**10:1 $[H_2O_2]$:[Ccp1]**
T4 VYNAIALK	891.5296	0.22	1.59E10 ± 7.12E8 **(4.5)**	1.50E10 ± 1.77E8 **(1.0)**	1.56E10 ± 8.57E08 **(5.5)**	1.66E10 ± 7.28E8 **(4.4)**
T19 TFFQR	698.3626	0.86	1.76E9 ± 7.80E7 **(4.4)**	1.78E9 ± 6.87E7 **(3.8)**	1.69E9 ± 8.50E7 **(5.0)**	1.76E9 ± 8.50E7 **(4.8)**
T27 YLSIVK	722.4450	0.41	1.30E9 ± 2.55E7 **(2.0)**	1.37E9 ± 4.51E7 **(3.3)**	1.32E9 ± 2.56E7 **(1.9)**	1.35E9 ± 7.20E7 **(5.3)**
T34 TLEEQGL	789.3993	0.50	1.59E9 ± 7.03E7 **(4.4)**	1.68E9 ± 9.67E7 **(5.7)**	1.66E9 ± 3.75E7 **(2.2)**	1.72E9 ± 6.79E7 **(3.9)**
Average ***PA*** of T4, T19, T27, T34 [d]			**5.1E9**	**5.0E9**	**5.1E9**	**5.4E9**

[a] No oxidative modifications were detected in these tryptic peptides, which are used as internal reference peptides.[3]

[b] The error in the observed monoisotopic *m/z* value in ppm is given by 10^6(Obs *m/z* – Calc *m/z*)/Calc *m/z*.

[c] The intensity of each peptide ion corresponds to its *PA* in the extracted ion chromatogram **(XIC)** within a 10 ppm exclusion window. Each *PA* is the average ± SD of four independent experiments (*n*=4) and the relative standard deviation (% RSD) is given in **red font**.

[d] The average *PA* at each H_2O_2:Ccp1 molar ratio is used as a normalization factor in Eq. 6 of the main text to correct for variation in instrument response and/or ion supression.[3]

Table S3: Monoisotopic *m/z* values of the MH^+ ions of tryptic peptides observed in the digests of H_2O_2-oxidzed Ccp1

Tryptic peptide [a]	Residues [a]	Residue(s) oxidized [b]	Obs MH^+ (*m/z*)	Calc MH^+ (*m/z*)	ppm error [c]
T2+T3	13-21	None	1129.5289	1129.5273	1.42
		Y16 (ox)	1145.5228	1145.5222	0.52
T3	15-21	None	916.4078	916.4047	3.38
		Y16 (ox)	932.4005	932.3996	0.97
T4	22-29	None	891.5310	891.5298	1.35
		Y23 (ox)	907.5249	907.5247	0.22
T5+T6	30-48	None	2286.1147	2286.1037	4.81
		Y42 (ox)	2302.1053	2302.0986	2.91
		Y39 (ox); Y42 (ox)	2318.0937	2318.0935	0.09
		Y36 (deH); Y39 (deH)	2284.0925	2284.0881	1.93
		Y39 (deH); Y42 (deH)	2284.0969	2284.0881	3.85
T6	32-48	None	2016.9206	2016.9185	1.04
		Y36 (ox)	2032.9174	2032.9134	1.97
		Y39 (ox)	2032.9200	2032.9134	3.25
		Y42 (ox)	2032.9172	2032.9134	1.87
		Y36 (deH); Y39 (deH)	2014.8979	2014.9029	-2.46
T7	49-59	None	1301.6290	1301.6273	1.31
		W57 (diox)	1333.6188	1333.6171	1.27
		W51 (diox); H52(ox)	1349.6158	1349.6121	2.74
		W51 (diox); W57 (diox)	1365.6086	1365.6069	1.24
		W51 (diox); W57 (diox); H52 (ox)	1384.6035	1384.6018	1.23
T8	60-72	None	1384.5857	1384.5876	-1.37
		Y71 (ox)	1400.5811	1400.5825	-1.00
		Y67 (ox); Y71 (ox)	1416.5842	1416.5775	4.73
		Y67 (deH); Y71 (deH)	1382.5776	1382.5720	4.05
T13	98-123	None	2780.3697	2780.3600	3.49
		M119 (ox)	2796.3589	2796.3549	1.43
		W101 (ox)	2796.3635	2796.3549	3.08
		W101 (ox); M119 (ox)	2812.3628	2812.3498	4.62
		W101 (diox); M119 (ox)	2828.3554	2828.3447	3.78
T14	124-127	None	571.3361	571.3351	1.75
		W126 (ox)	587.3308	587.3300	1.36
T14+T15	124-130	None	887.4668	887.4669	-0.11
		W126 (ox); C128 (diox)	935.4524	935.4516	0.86
		W126 (ox); C128 (triox)	951.4455	951.4465	-1.05
		W126 (diox); C128 (triox)	967.4446	967.4414	3.31
T16+T17+T18	131-155	None	2775.2782	2775.2704	2.81
T17+T18	144-155	None	1377.6588	1377.6645	-4.14
T20	161-166	None	762.3591	762.3563	3.67
		M163 (ox)	778.3529	778.3512	2.18
T20+T21	161-179	None	2039.0542	2039.0525	0.83
		M163 (ox)	2055.0475	2055.0474	0.05
		M172 (ox); H175 (ox)	2071.0429	2071.0423	0.29
T21	167-179	None	1295.7149	1295.7140	0.69
		M172 (ox)	1311.7099	1311.7089	0.76
		H175 (ox)	1311.7060	1311.7089	-2.21

		M172 (ox); H175 (ox)	1327.7065	1327.7038	2.03
T23	184-212	None	3362.5536	3362.5389	4.37
		W191 (ox)	3378.5398	3378.5338	1.78
		W211 (ox)	3378.5353	3378.5338	0.44
		W191 (ox); W211 (diox)	3410.5275	3410.5236	1.14
T23+T24	184-215	None	3732.7527	3732.7605	-2.09
		W211 (ox)	3748.7640	3748.7554	2.30
		W191 (ox); W211 (diox)	3780.7540	3780.7453	2.30
		W191 (diox); W211 (diox)	3796.7544	3796.7401	3.77
T24+T25	213-226	None	1690.7642	1690.7667	-1.48
		W223 (ox)	1706.7592	1706.7616	-1.41
		W223 (diox)	1722.7558	1722.7565	-0.41
		W223 (kyn)	1694.7630	1694.7616	0.83
T25	216-226	None	1320.5460	1320.5451	0.68
		W223 (ox)	1336.5402	1336.5400	0.15
		W223 (diox)	1352.5354	1352.5349	0.37
T25+T26	216-243	None	3260.4611	3260.4511	3.07
		W223 (ox)	3276.4603	3276.4460	4.36
		Y229 (deH); Y236 (deH)	3258.4475	3258.4355	3.68
		Y229 (deH); Y236 (deH); M230 (ox)	3274.4412	3274.4304	3.30
		W223 (ox); M230 (ox); M231 (ox)	3308.4425	3308.4358	2.03
T26	227-243	None	1958.9296	1958.9238	2.96
		Y229 (ox)	1974.9265	1974.9187	3.95
		M230 (ox); M231 (ox)	1990.9207	1990.9136	3.57
		Y229 (ox); M230 (ox)	1990.9192	1990.9136	2.81
		Y229 (deH); Y236 (deH)	1956.9138	1956.9074	3.27
		Y229 (deH); Y236 (deH); M230 (ox)	1972.9081	1972.9031	2.53
T27	244-249	None	722.4450	722.4447	0.42
		Y244 (ox)	738.4380	738.4396	-2.17
		Y244 (diox)	754.4352	754.4345	0.93
T28	250-257	None	982.4110	982.4112	-0.20
		Y251 (ox)	998.4077	998.4061	1.60
T28+T29	250-260	None	1404.6479	1404.6430	3.49
		Y251 (ox)	1420.6410	1420.6379	2.18
T28+T29+T30	250-264	None	1881.8700	1881.8654	2.44
		Y251 (ox)	1897.8605	1897.8603	0.11
		Y251 (diox)	1913.8564	1913.8552	0.63

[a] Fig. S1 gives the tryptic map of Ccp1 and the sequence of tryptic peptides T1-T34.

[b] Observed residue modifications are assigned based on the Δm values in Table S1.

[c] See definition of ppm error in Footnote b of Table S2.

Table S4: CCP activity of H_2O_2-oxidized Ccp1 [a]

$[H_2O_2]$:[Ccp1] [b]	CCP activity [a]	Percent activity [c]
0:1	1.70 ± 0.010	100 ± 0.00
0.5:1	1.59 ± 0.021	93.5 ± 0.93
1:1	1.34 ± 0.045	78.8 ± 2.37
3:1	0.92 ± 0.028	54.1 ± 2.16
5:1	0.66 ± 0.036	38.8 ± 3.88
10:1	0.18 ± 0.008	10.6 ± 3.30

[a] One unit of CCP activity catalyzes the oxidation by H_2O_2 of 1 µmol of horse heart ferrocytochrome c (Cyc^{II}) per min per mg Ccp1.

[b] Stock Ccp1 (5 µM) and H_2O_2 solutions (0.01–1 mM) were prepared in Kpi/DTPA, and mixed to give 1 µM Ccp1 with the desired H_2O_2 concentrations. Samples were incubated at room temperature for 1 h and activities were measured as described previously.[4] For the assay, a stock solution of Cyc^{III} was ~90% reduced with sodium dithionite and the Cyc^{II} concentration determined spectrophotometrically (ε_{550} = 27.6 mM^{-1} cm^{-1}).[5]

[c] The activity of each fraction was ratioed by the activity of the 0:1 sample to give percent activity. Results are presented as averages ± SD from three independent experiments (*n*=3).

Table S5. Peptides T21 (M172, H175) and T14+T15 (W126, C128) are oxidized at two residues [a]

Tryptic peptide	Residue(s) oxidized (X_{ox})	Obs MH^+ (m/z)[b]	Calc MH^+ (m/z)[c]	ppm error [c]	% X_{ox} [d]			
					H_2O_2:Ccp1			
					0:1	1:1	5:1	10:1
T21	None	1295.7149	1295.7140	0.70	90.9 ± 0.1	66.4 ± 10.2	17.5 ± 1.0	9.2 ± 1.4
T21	M172 +16	1311.7108	1311.7089	1.44	8.8 ± 11.1	30.4 ± 2.9	47.2 ± 5.7	48.2 ± 3.1
T21	H175 +16	1311.7050	1311.7089	-2.97	---	3.2 ± 2.5	28.5 ± 2.0	37.2 ± 3.2
T21	M172 +16, H175 +16	1327.7064	1327.7038	1.95	---	---	6.8 ± 4.0	4.9 ± 0.5
T14+T15	None	887.4668	887.4669	-0.11	100 ± 0.0	96.8 ± 0.6	3.7 ±2.6	1.9 ± 3.7
T14+T15	W126+16, C128 +32	935.4524	935.4516	0.85	---	---	23.7 ± 5.3	45.0 ± 2.7
T14+T15	W126 +16, C128 +48	951.4455	951.4465	-1.05	---	---	33.6 ± 6.9	48.2 ± 1.4
T14+T15	W126 +32, C128 +48	967.4446	967.4414	3.30	---	---	2.2 ± 0.7	5.2 ± 1.3

[a] Ccp1 (1 µM) was reacted with 1, 5 and 10 M eq of H_2O_2 for 1 h at room temperature in KPi/DTPA prior to tryptic digestion and LC-MS/MS analysis as described on page 3 of the SI.

[b] The precursor ions selected for MS2 analysis were filtered using a mass exclusion threshold of 10 ppm.

[c] The monoisotopic *m/z* values for the peptide MH^+ ions were calculated using Protein Prospector (http://prospector.ucsf.edu), and the ppm errors were calculated as in Footnote b of Table S2.

[d] The percent oxidation of H175, M172, W126 and C128 was calculated using Eq. 6 of the main text.

Table S6: Assignment of sequence ions in the MS/MS spectrum of the T6 native peptide [a]

#1[c]	b^+	b^{2+}	b^{3+}	Seq.[b]	y^+	y^{2+}	y^{3+}	#2[c]
1	130.04988	65.52858	44.02148	E				17
2	245.07683	123.04205	82.36379	D	1887.87599	944.44163	629.96351	16
3	360.10378	180.55553	120.70611	D	1772.84904	886.92816	591.62120	15
4	489.14638	245.07683	163.72031	E	1657.82209	829.41468	553.27888	14
5	652.20970	326.60849	218.07475	Y	1528.77949	764.89338	510.26468	13
6	767.23665	384.12196	256.41707	D	1365.71617	683.36172	455.91024	12
7	881.27958	441.14343	294.43138	N	1250.68922	625.84825	417.56792	11
8	1044.34290	522.67509	348.78582	Y	1136.64629	568.82678	379.55361	10
9	1157.42697	579.21712	386.48051	I	973.58297	487.29512	325.19917	9
10	1214.44844	607.72786	405.48766	G	860.49890	430.75309	287.50448	8
11	1377.51176	689.25952	459.84210	Y	803.47743	402.24235	268.49733	7
12	1434.53323	717.77025	478.84926	G	640.41411	320.71069	214.14289	6
13	1531.58600	766.29664	511.20018	P	583.39264	292.19996	195.13573	5
14	1630.65442	815.83085	544.22299	V	486.33987	243.67357	162.78481	4
15	1743.73849	872.37288	581.91768	L	387.27145	194.13936	129.76200	3
16	1842.80691	921.90709	614.94049	V	274.18738	137.59733	92.06731	2
17				R	175.11896	88.06312	59.04450	1

[a] Observed b_n and y_n sequence ions in spectrum A of Fig. 6 of the main text.

[b] Sequence of T6 peptide - EDDEYDNYIGYGPVLVR

[c] Ions highlighted in **red** and **blue** font are b_n and y_n sequence ions, respectively, identified by MS/MS. Sequence ions in black are not identified by MS/MS. The sequence assignment is based on residue masses at 0.8 u mass tolerance (see page 3 of the SI for the experimental details).

Table S7: Assignment of sequence ions in the MS/MS spectrum of the T6 oxidized peptide [a]

#1[c]	b^+	b^{2+}	b^{3+}	Seq.[b]	y^+	y^{2+}	y^{3+}	#2[c]
1	130.04988	65.52858	44.02148	E				17
2	245.07683	123.04205	82.36379	D	1885.86034	943.43381	629.29163	16
3	360.10378	180.55553	120.70611	D	1770.83339	885.92033	590.94931	15
4	489.14638	245.07683	163.72031	E	1655.80644	828.40686	552.60700	14
5	651.20187	326.10457	217.73881	Y-Dehydro	1526.76384	763.88556	509.59280	13
6	766.22882	383.61805	256.08112	D	1364.70835	682.85781	455.57430	12
7	880.27175	440.63951	294.09543	N	1249.68140	625.34434	417.23198	11
8	1042.32725	521.66726	348.11393	Y-Dehydro	1135.63847	568.32287	379.21767	10
9	1155.41132	578.20930	385.80862	I	973.58297	487.29512	325.19917	9
10	1212.43279	606.72003	404.81578	G	860.49890	430.75309	287.50448	8
11	1375.49611	688.25169	459.17022	Y	803.47743	402.24235	268.49733	7
12	1432.51758	716.76243	478.17738	G	640.41411	320.71069	214.14289	6
13	1529.57035	765.28881	510.52830	P	583.39264	292.19996	195.13573	5
14	1628.63877	814.82302	543.55111	V	486.33987	243.67357	162.78481	4
15	1741.72284	871.36506	581.24580	L	387.27145	194.13936	129.76200	3
16	1840.79126	920.89927	614.26860	V	274.18738	137.59733	92.06731	2
17				R	175.11896	88.06312	59.04450	1

[a] Observed b_n and y_n sequence ions in spectrum B of Fig. 6 of the main text.

[b,c] See Footnotes b and c to Table S6.

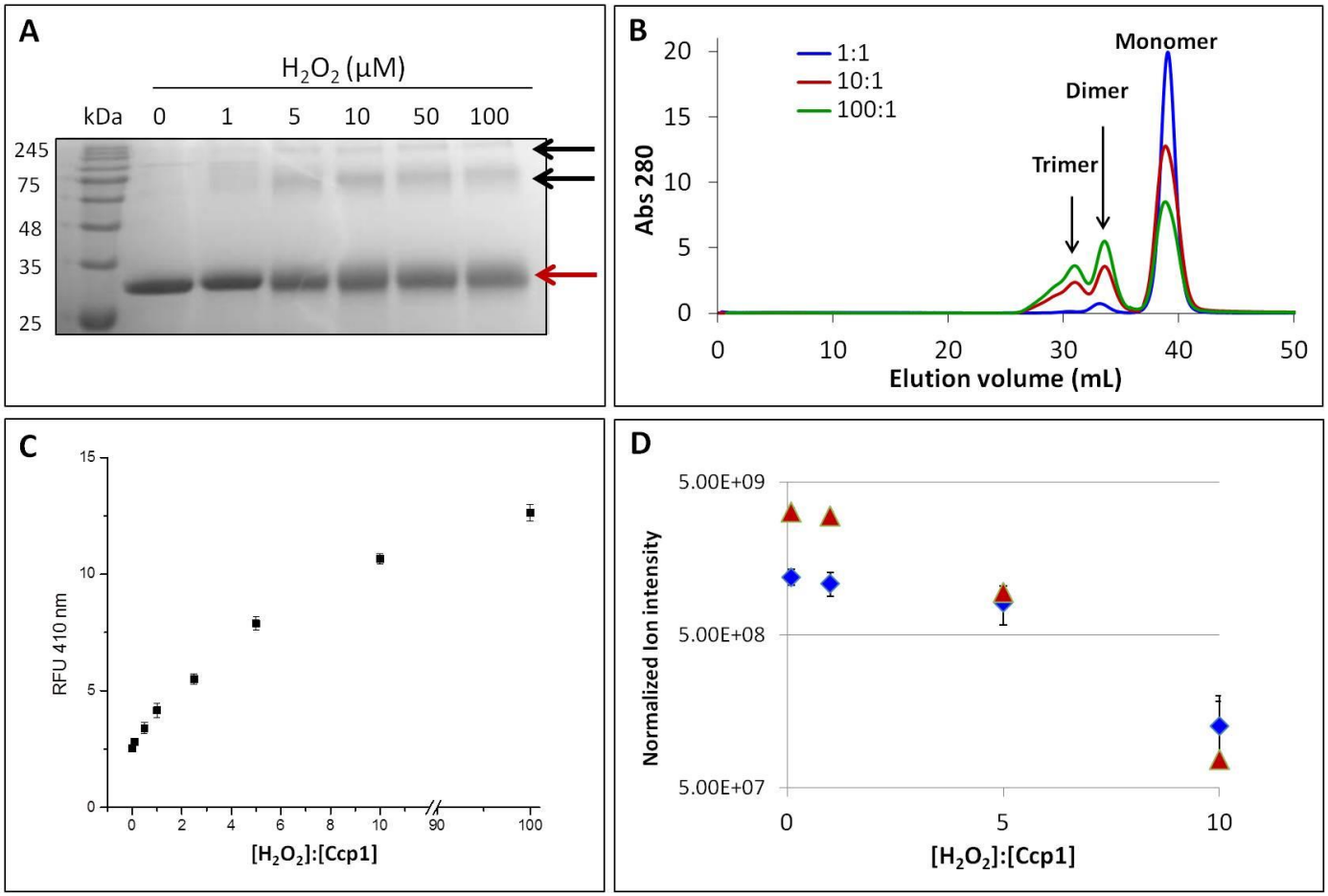

Fig. S2: Characterization of *intramolecular* dityrosine crosslinks in H_2O_2-oxidized Ccp1

(A) SDS-PAGE analysis of H_2O_2-oxidized Ccp1 under reducing conditions. Ccp1 (1 µM) was treated with the indicated H_2O_2 concentration in KPi/DTPA for 1 h at room temperature and analyzed by 12% SDS-PAGE followed by Coomassie staining. The red arrow indicates that Ccp1 is predominantly monomeric (~35 kDa) but small quantities of the dimer and trimer (~70 and ~100 kDa) can be detected in the samples treated with 5-100 µM H_2O_2. The band containing monomeric Ccp1 becomes noticeably more diffuse with increasing H_2O_2 added indicative of increased protein modification. **(B)** Gel-filtration chromatography of H_2O_2-oxidized Ccp1. Stock solutions in KPi/DTPA were mixed to give 10 µM Ccp1 with 10, 100 and 1000 µM H_2O_2, and incubated for 1 h at room temperature. Aliquots (100 µL) were applied to a 24-mL Superdex 200 HR 10/30 column (fractionation range 10-600 kDa) equilibrated with 20 mM KPi pH 7.5/150 mM NaCl and coupled to an ÄKTApurifier 10 (GE) with 280-nm detection. The protein was eluted in equilibration buffer at a flow rate of 0.5 mL/min and fractions containing monomeric Ccp1 were collected. Note that 10 µM Ccp1 was oxidized in order to obtain sufficient sample for the gel-filtration analysis but only 1 µM Ccp1 was oxidized for the MS analyses to attenuate *intermolecular* crosslinking as discussed in the Experimental section of the main text. **(C)** The monomeric Ccp1 samples were diluted to 1 µM in KPi/DTPA and on excitation at 315 nm, their emission at 410 nm was recorded in a Cary Eclipse fluorometer with 5-nm slits. Relative fluorescence units (RFU) are from three independent experiments (n=3) and averages ± SD are plotted. **(D)** Normalized ion intensity across three replicates for T6 (Y36, Y39, Y42; blue diamonds) and T8 (Y67, Y71; red triangles) plotted vs H_2O_2:Ccp1 molar ratio.

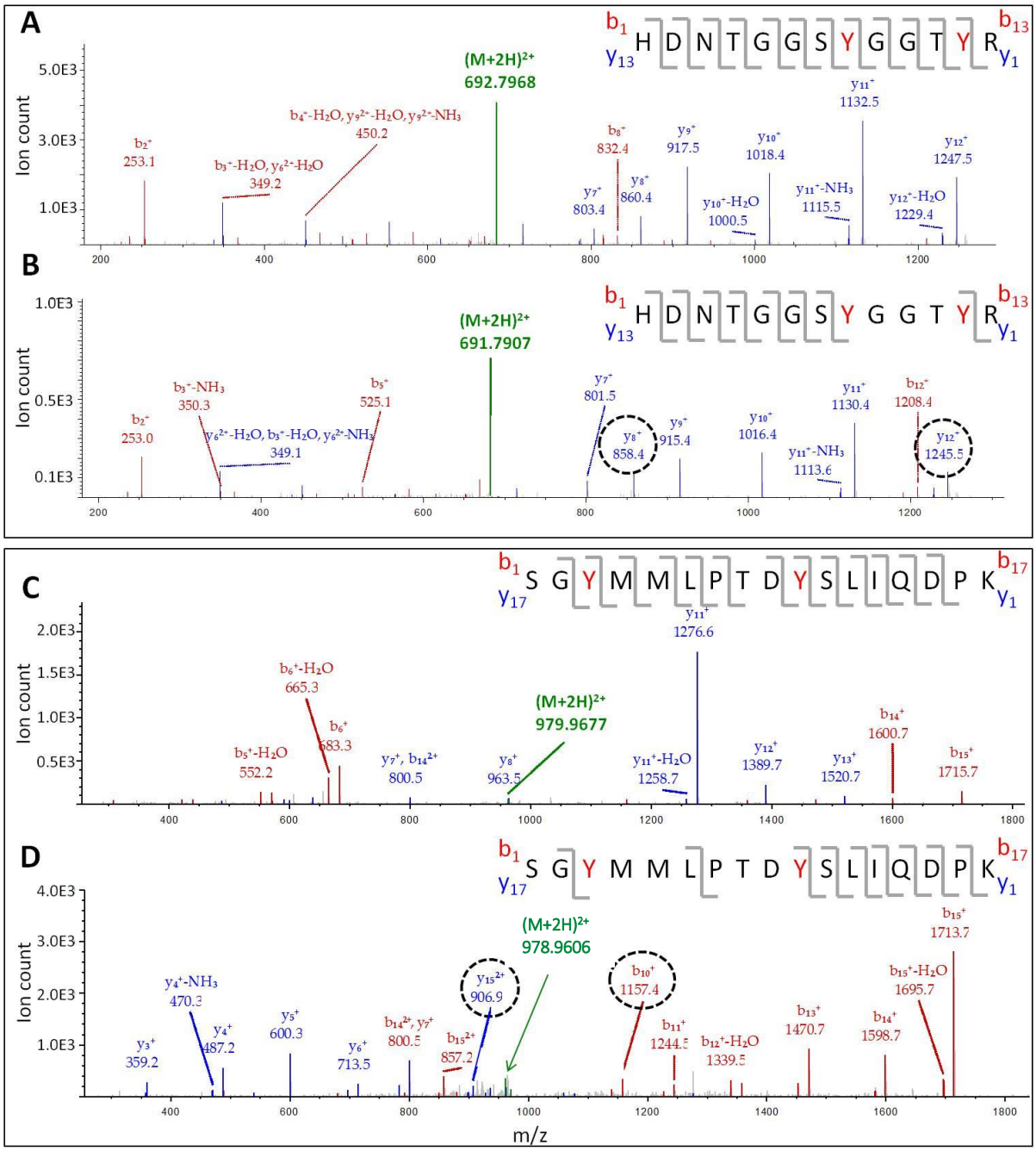

Fig. S3. LC-MS/MS analysis of dityrosine formation in tryptic peptides T8 and T26

MS2 spectrum of the $(M+2H)^{2+}$ ion of: **(A)** native T8 at *m/z* 692.7968; **(B)** oxidized T8 at *m/z* 691.7907; **(C)** native T26 at *m/z* 979.9677; and **(D)** oxidized T26 at *m/z* 978.9606. The T8 and T26 precursor ions (green) were fragmented by CID (30 V) to give b_n (red) and y_n (blue) sequence ions. The encircled y_8^+/y_{12}^+ ions in panel B and b_{10}^+/y_{15}^{2+} ions in panel D have masses consistent with loss of an H atom (-1 u) from Y67/Y71 and Y229/Y236, respectively. For panels C and D, we selected peaks that do not contain T26 oxidized at M230 or M231 for clarity. The peptide sequence in each panel shows the tyrosines in red font and the observed fragmentations are mapped onto the sequence. Note the absence of fragmentation between crosslinked Y67 and Y71 (panel B), and the single fragmentation within the large 8-residue loop formed by the Y229-Y236 crosslink (panel D).

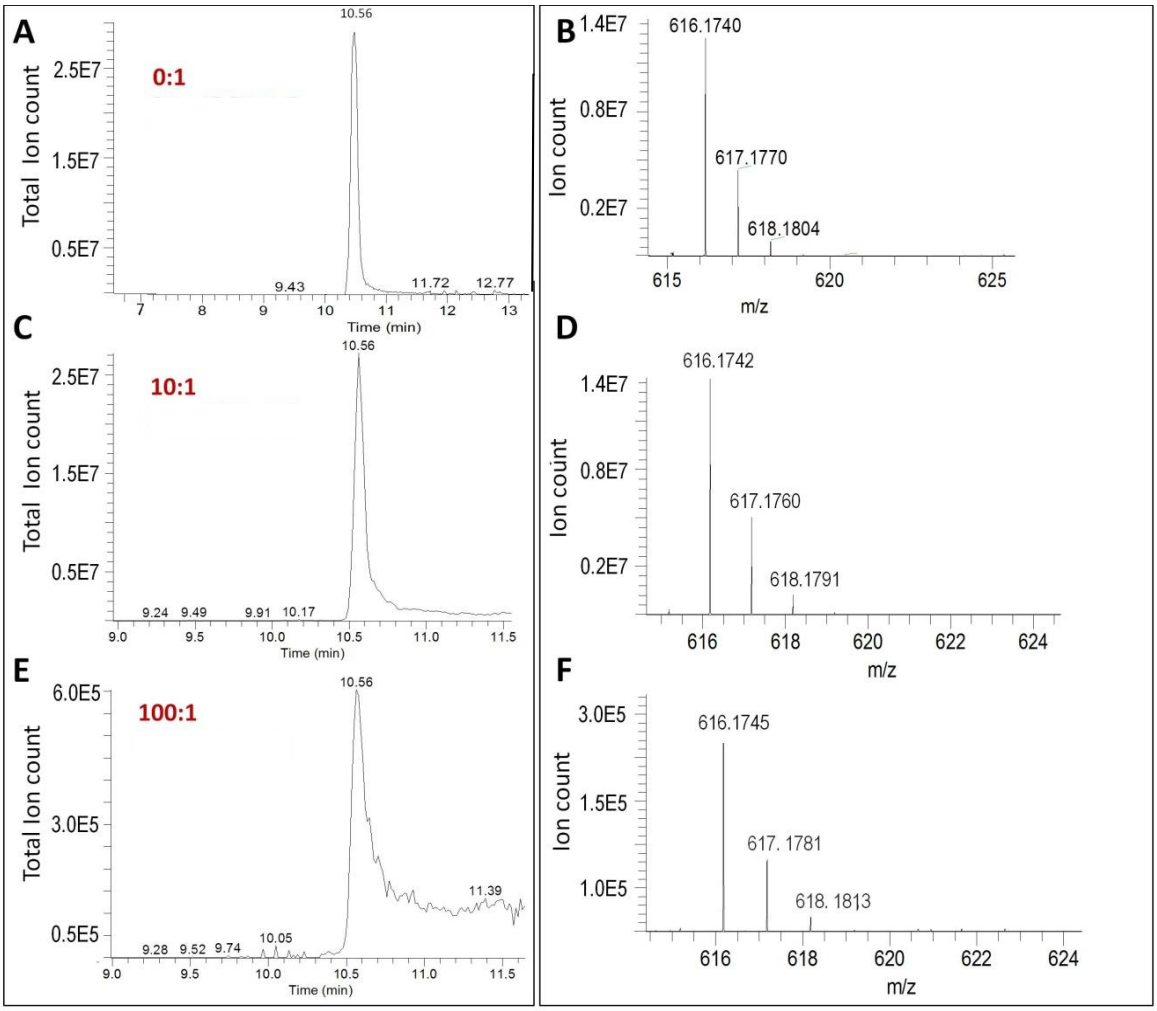

Fig. S4: LC-MS analysis of hemin released from Ccp1 exposed to 0, 10 and 100 M eq of H_2O_2

Following oxidation of 1 µM Ccp1 by 0, 10 and 100 µM H_2O_2 in KPi/DTPA for 1 h at room temperature, samples were diluted 10-fold into the MS solvent and 5-µL aliquots were analyzed by LC-MS (see page 3 of the SI). **(A,C,E)** Chromatograms showing the peak at 10.56 ± 0.02 min containing hemin that dissociated from Ccp1 on the C4 column at pH 4.0. The H_2O_2:Ccp1 molar ratio is indicated in **red font** on the figures. **(B,D,F)** The corresponding hemin mass spectrum showing the isotopic distribution expected for the M^+ ion ($FeC_{34}H_{22}N_4O_4$; calc mass 616.1773 u). The exact mass of hemin released from Ccp1 is 616.1742 ± 0.00025 u compared to 616.1746 u for authentic hemin, which was used as an external standard. Note the ~100-fold lower total ion count (y-axis) in panels E,F vs panels A,B,C,D which reflects the extensive destruction of Ccp1's heme by 100 M eq of H_2O_2, whereas negligible loss of heme is seen following oxidation of Ccp1 with 10 M eq of H_2O_2.

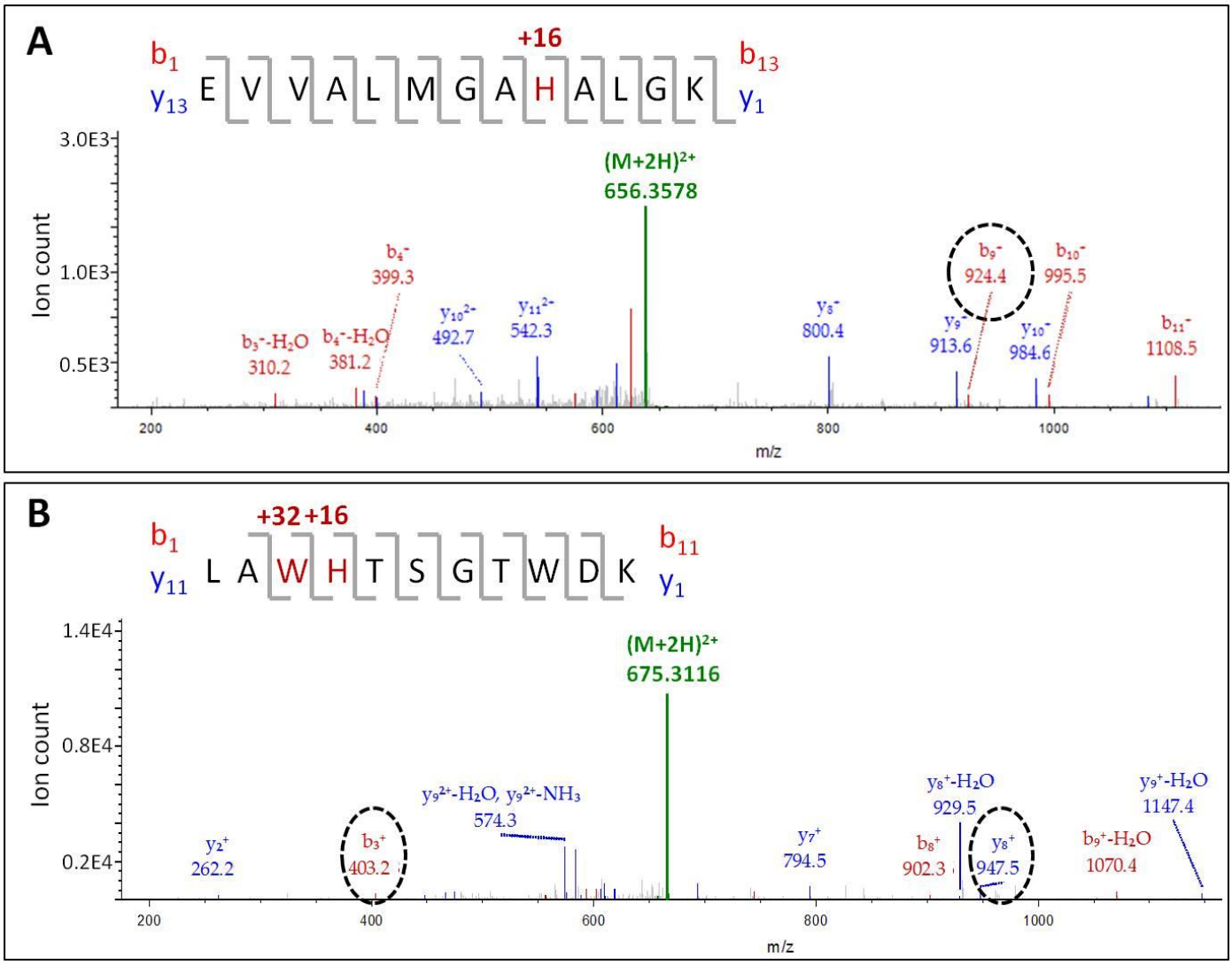

Fig. S5: LC-MS/MS analysis of H175 and H52 oxidation in tryptic peptides T21 and T7

The MS2 spectrum of the $(M+2H)^{2+}$ ion of: **(A)** T21 with oxidized H175 at *m/z* 656.3578; and **(B)** T7 with oxidized H52 at *m/z* 675.3116. The T21 and T7 precursor ions (green) were fragmented by CID (30 V) to give b_n (red) and y_n sequence ions (blue). The encircled b_9^+ and y_8^+ ions have masses consistent with addition of an oxygen atom (+16 u) to both H175 and H52. Also, the mass of the encircled b_3^+ ion in panel B indicates the addition of two oxygen atoms (+32 u) to W51. The observed fragmentations are mapped onto the sequence. See page 3 of the SI for the experimental details.

Standard MD simulations of Ccp1 in water with O_2 molecules

The crystal structure of Ccp1 (1ZBY)[6] was chosen as the initial structure for all-atom MD simulations. The positions of the side-chain O and N atoms in Asn and Gln residues, and the protonation states of His, Asp and Glu residues were established by examining the surrounding protein environment. Note that all the oxidizable residues in Fig. S6 are in the neutral form except H60 and H181, which are protonated. Conformer A was selected for residues R48, K123, D152, R166, M172, A193, A194, N195, D210, S246 and K287. Conserved internal crystal water 770 was removed to prevent steric clashing with R48. The remaining 836 crystal waters were embedded with Ccp1 in a box of TIP3P water molecules[7] to provide a water layer of > 8 Å around the protein. Sodium and chloride ions were added to ensure charge neutrality and to set the NaCl concentration to 0.15 M. Ten or 100 O_2 molecules were added into the box outside the protein, and the resulting system was simulated using periodic boundary conditions.

MD simulations were performed with the NAMD 2.7 program[8] using the CHARMM36 all-atom force field[9] at a constant temperature of 310 K and a constant pressure of 1 atm. The van der Waals parameters for the O atom (ε = -0.12 kcal/mol, $R_{min}/2$ =1.7Å) were taken from the CHARMM36 force field,[3] and the published experimental O-O bond length (l =1.207Å) and its vibrational frequency (1580.19 cm^{-1})[10] were used to calculate the O-O bond force constant (k =1693 kcal/mol/$Å^2$). The particle-mesh Ewald method[11] with a grid size of < 1 Å was selected for long-range electrostatics, while a cut-off of 12 Å was assumed for all other non-bonded interactions. Van der Waals interactions were truncated at a distance of 8 Å using a switching function, and bonds involving hydrogen atoms were constrained using the SHAKE algorithm,[12] permitting the use of a multiple time-step algorithm[13] to compute bonded and short-range non-bonded interactions every 2 fs and long-range electrostatic forces every 6 fs. The temperature and pressure were controlled using Langevin dynamics with the Langevin piston Nose-Hoover method and a damping coefficient γ of 5 ps^{-1}.[14,15] The system was heated over 0.4 ns and equilibrated over 1.1 ns, gradually removing the initial restraints on the C_α-backbone atoms and the O atoms of the internal water molecules. Then, a productive run of ~32 ns was performed and only productive runs were analyzed.

In total, 7 independent 32-ns standard trajectories with 10 or 100 O_2 molecules were obtained. The size of the periodic box was ~76x76x76 $Å^3$ after equilibration, giving O_2 concentrations of ~ 38 and ~380 mM in simulations with 10 and 100 O_2 molecules, respectively, which are > 10^2-10^3-fold higher that of O_2 in water at 293 K and 1 atm (~0.3 mM). These high O_2 concentrations significantly increased sampling of the O_2 docking sites on the surface of Ccp1 and similar results were obtained with 10 or 100 O_2 molecules, but the more intense sampling in simulations with 100 O_2 molecules lead to better convergence. Therefore, the results for simulations with 100 O_2 molecules are shown in Fig. S6, which was produced with the VMD package.[16] Notably, the largest O_2 docking sites are present in hydrophobic grooves on the surface of Ccp1 near H96 and M119, and other surface docking sites are found in hydrophobic patches near Y16, Y42, W101, Y153, Y187, W223, Y236 and Y251. Buried O_2 docking sites, such as the cluster around the distal H52 tend to be smaller than the surface sites due to steric constrains.

From Table S8, we can see that many (15/24) of the residues found to be oxidized in Ccp1 are within 5 Å of an O_2 docking site, which will promote O_2 trapping of radicals formed on these residues. During the simulations, most of the internal waters remained close to their positions in the crystal structure of Ccp1. Strikingly, 26 of the 31 conserved internal waters are located in the distal domain (Fig. S6, Table S8). However, all of Ccp1's oxidizable residues are either solvent exposed or within 5 Å of an internal water molecule. The thermodynamics of one-electron oxidation of most residues require proton transfer at physiological pH (with the rare exception of W191). This is facilitated in Ccp1 by water accessibility to its oxidizable residues,

which underscores the physiological significance of these residues as donors to the heme when Ccp1's reducing substrate, Cyc^{II} (Eqs 2,3 of the main text), is unavailable. We note that simulations were performed using the structure of resting, unoxidized Ccp1. Oxidation will most likely alter the structure of the protein and possibly increase water and oxygen accessibility to its buried residues. However, the CD spectra shown in Fig. S7 reveal little change in Ccp1's secondary structure even after its oxidation by 10 M eq of H_2O_2.

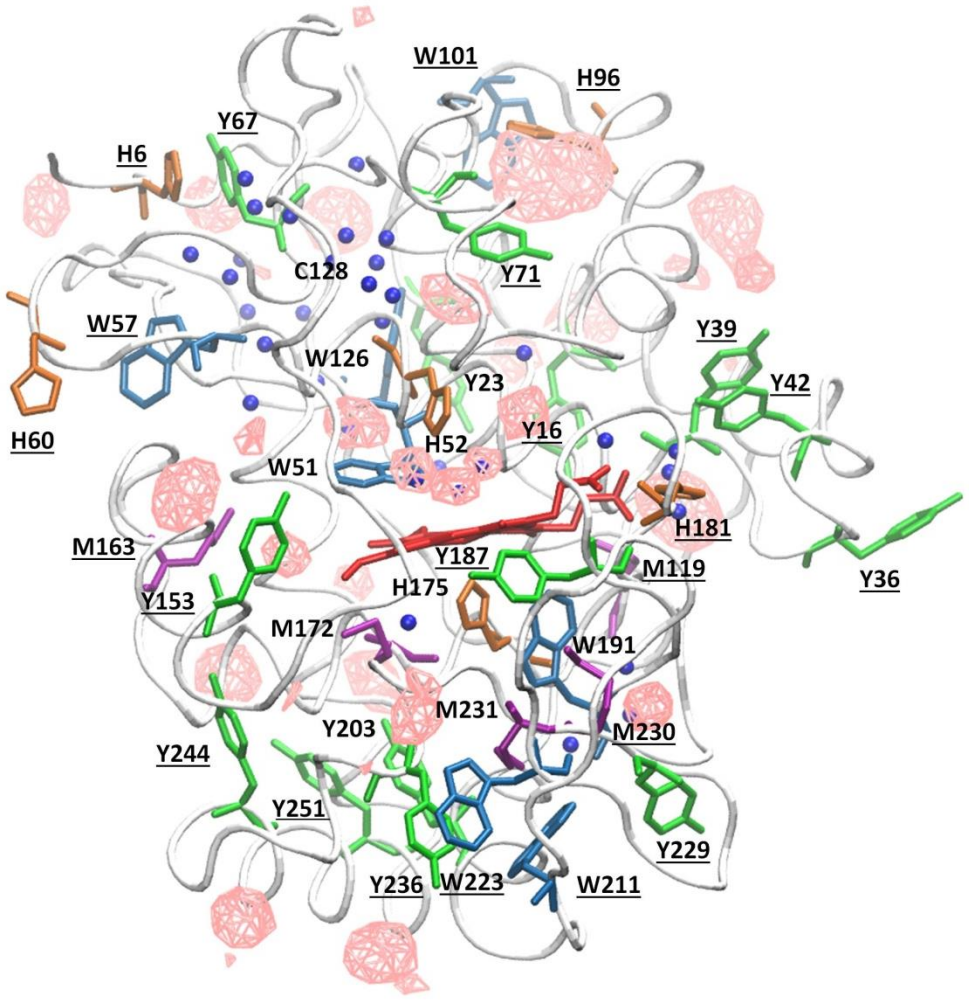

Fig. S6: MD simulation of Ccp1 in water with 100 added O_2 molecules

VMD-generated[16] cartoon of Ccp1 (PDB 1ZBY) showing all 33 oxidizable residues (W, blue; Y, green; H, orange; M, purple, C, grey) and those solvent-exposed are underlined. Blue spheres locate the 31 conserved internal water molecules (517, 518, 519, 520, 525, 526, 527, 528, 531, 542, 543, 547, 548, 549, 552, 576, 578, 605, 640, 644, 645, 655, 656, 663, 692, 693, 696, 697, 698, 895, 1232), which were found in 11 PDB structures (1MKQ, 1CCA, 1RYC, 1ZBY, 2XIL, 2XJ5, 2XJ8, 2YCG, 4A6Z, 4A71, 4P4Q), including those of CpdI and CpdII (underlined). Average O_2 densities from 7 standard MD simulations of ~32 ns duration of Ccp1 with 100 O_2 molecules are shown as pink wire surfaces, which represent favorable O_2 docking sites in the polypeptide. The number of such O_2 sites and the number of conserved internal waters found within 5 Å of each oxidizable residue are listed in Table S8.

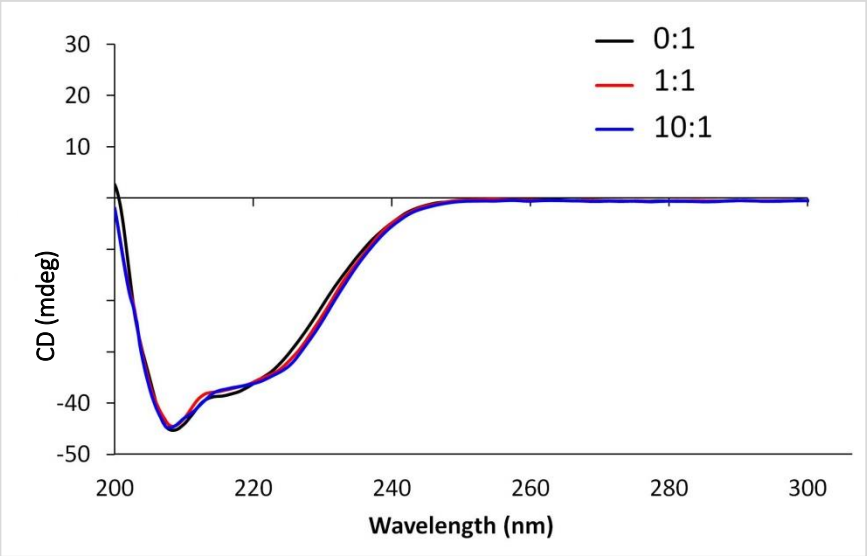

Fig. S7: Ultraviolet circular dichroism spectrum of Ccp1 oxidized with 0, 1 and 10 M eq of H_2O_2

An aliquot of holoCcp1 was mixed with 0 (black line), 1 (red line) and 10 M eq of H_2O_2 (blue line) in 20 mM KPi buffer (pH 7.5) in an 0.5-cm pathlength cuvette at room temperature for 1 h before recording the CD spectra. The final concentration of Ccp1 was 2.5 µM. The absorbance below 240 nm reveals little change in secondary structure on oxidation of Ccp1 with H_2O_2.

Table S8: O_2 and water exposure of the oxidizable residues in Ccp1 [a]

Residue	Oxidation level [b,c]	O_2 docking sites < 5 Å [d]	Conserved internal waters < 5 Å [d]	H-bonding to water [e]	Solvent exposed [f]	Zone [g]
M119	H	1			yes	3
M163	M	0	W520		yes	4
M172	H	1	W605	yes		3
M230	H	0			yes	1
M231	H	0		yes		1
C128	H	3	W549, W656	yes		2
H6	ND	0			yes	NA
H52	H	3	W640, W643, W1232	yes		3
H60	ND	0			yes	NA
H96	ND	1			yes	NA
H175	H	0	W578, W605	yes		3
H181	ND	0			yes	NA
W51	H	2	W640, W1232	yes		3
W57	H	0	W520	no	yes	2a
W101	L	1			yes	2a
W126	H	2	W543, W547, W655	no		2a
W191	H	0	W578	yes		1
W211	H	1			yes	1
W223	H	1			yes	1
Y16	M	1			yes	2a
Y23	ND	0	W543	no		NA
Y36	H (-1)	0	W517, W692	yes	yes	2b
Y39	H (-1)	0			yes	2b
Y42	H (-1)	1	W517	no	yes	2b
Y67	H (-1)	1	W552, W697, W698	yes	yes	2a
Y71	H (-1)	1	W645	yes	yes	2a
Y153	ND	1			yes	4
Y187	ND	1			yes	NA
Y203	ND	0	W576	no		4
Y229	H / L (-1)	0			yes	1
Y236	L (-1)	1			yes	1
Y244	ND	0			partially	4
Y251	L	1			partially	4

[a] The 33 oxidizable residues in Ccp1 (see Fig. 1 of the main text and Fig. S6)

[b] The oxidation level of a given residue is classified as high (H: 40-100%), medium (M: 20-40%), low (L: 5-20%) or not detectable (ND) based on the oxidation yields calculated using Eq. 6 of the main text.

[c] Oxidized residues incorporated 1-3 oxygen atoms or lost a hydrogen atom (Table S3) where indicated (-1).

[d] Number of O_2 docking sites and conserved internal waters within 5 Å of the side chain of the indicated residue (Fig. S6).

[e] H-bonding is assumed if the oxygen atom of an internal water and a residue heteroatom are within 3 Å.

[f] Solvent exposure is based on accessibility of bulk water.

[g] See donor zones in Fig. 8 of the main text.

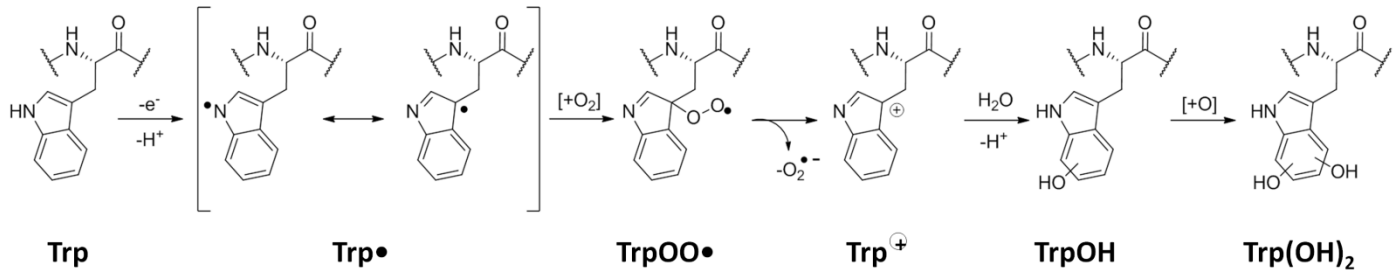

Scheme S1: Proposed pathway of tryptophan oxidation

One-electron oxidation of tryptophan (Trp) yields the tryptophanyl radical (Trp•, **W•**), which reacts with dioxygen to give the tryptophan peroxyl radical (TrpOO•).[17] Superoxide release and water capture by the aryl carbocation leads to TrpOH, which can be further oxidized to $Trp(OH)_2$.[18]

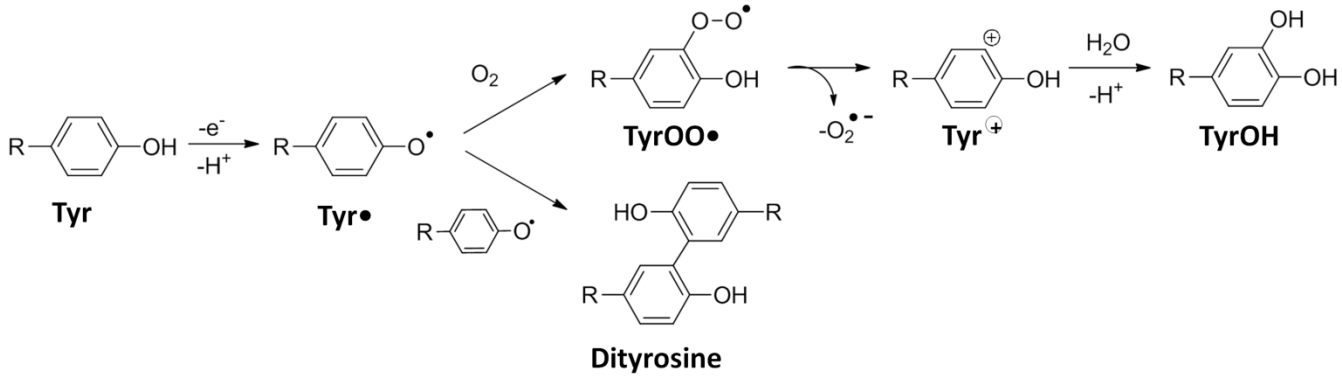

Scheme S2: Proposed pathway of tyrosine oxidation

One-electron oxidation of tyrosine (Tyr) yields a tyrosyl radical (Tyr•, **Y•**), which reacts rapidly with a second Tyr• to form dityrosine.[19] In the absence of a second Tyr•, the radical reacts slowly with dioxygen to form the tyrosine peroxyl radical (TyrOO•).[20] Superoxide release and water capture by the aryl carbocation leads to TyrOH.

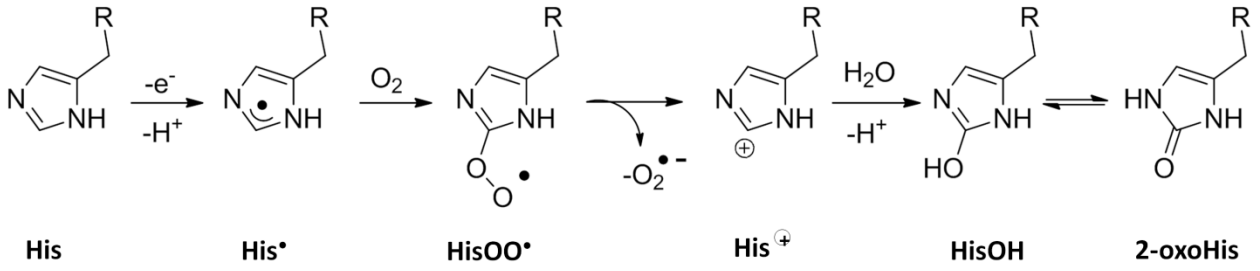

Scheme S3: Proposed pathway of histidine oxidation

One-electron oxidation of histidine (His) yields a histidine radical (His•, **H•**), which reacts with dioxygen to give the histidine peroxyl radical (HisOO•).[21] Superoxide release and water capture by the aryl carbocation leads to HisOH. The C-2 adduct of the imidazole ring is the energetically most stable species, forming 2-oxoHis.[22]

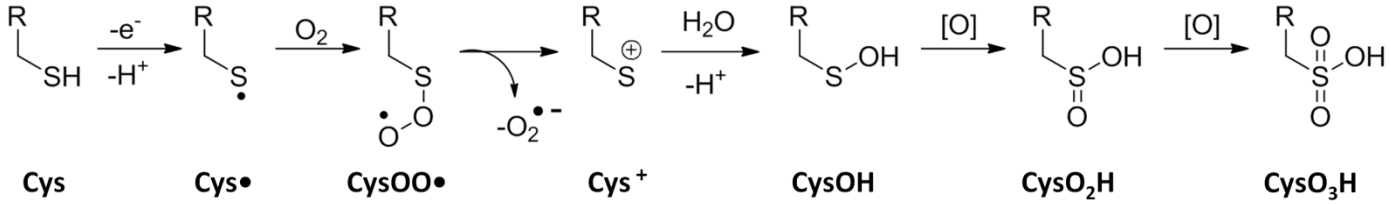

Scheme S4: Proposed pathway of cysteine oxidation

One-electron oxidation of cysteine (Cys) yields a sulfur radical cation[23] that deprotonates to give the cysteinyl radical (Cys•, **C•**). This reacts rapidly with dioxygen (6.1 x10^7 $M^{-1}s^{-1}$)[24] to give the cysteine peroxyl radical (CysSOO•).[25,26] Superoxide release and water capture will give CysOH, which can be further oxidized to $CysO_2H$ and $CysO_3H$.

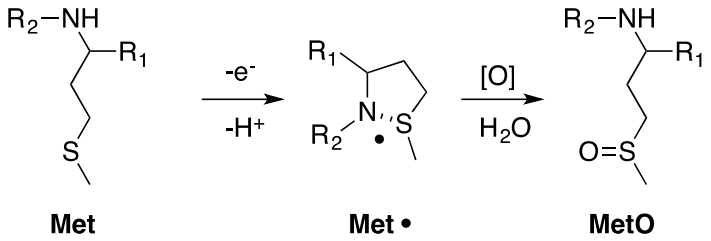

Scheme S5: Proposed pathway of methionine oxidation

One-electron oxidation of methionine (Met) yields a sulfur radical, which may be stabilized by ring formation between the sulfur and the amino group.[27,28] The subsequent one-electron oxidation of Met• by dioxygen will generate methionine sulfoxide (MetO) on water capture. [27,28] As proposed for heme-mediated methionine oxidation in MauG, a protein-based transient Met• may be stabilized by ring formation involving a two-center, three-electron (2c3e) bond between the sulfur and a neighboring amide nitrogen or oxygen or an aromatic group.[29]

Supplemental literature cited

1 E. R. Stadtman, *Annu Rev Biochem*, 1993, **62**, 797–821.

2 I. M. Møller, A. Rogowska-Wrzesinska and R. S. P. Rao, *J Proteomics*, 2011, **74**, 2228–2242.

3 S. D. Sherrod, M. V Myers, M. Li, J. S. Myers, K. L. Carpenter, B. Maclean, M. J. Maccoss, D. C. Liebler and A. L. Ham, *J Proteome Res*, 2012.

4 M. Kathiresan, D. Martins and A. M. English, *Proc Natl Acad Sci U S A*, 2014, **111**, 17468–17473.

5 T. Yonetani, *J Biol Chem*, 1965, **240**, 4509–4514.

6 C. A. Bonagura, B. Bhaskar, H. Shimizu, H. Li, M. Sundaramoorthy, D. E. McRee, D. B. Goodin and T. L. Poulos, *Biochemistry*, 2003, **42**, 5600–5608.

7 W. L. Jorgensen, J. Chandrasekhar, J. D. Madura, R. W. Impey and M. L. Klein, *J Chem Phys*, 1983, **79**, 926–935.

8 J. C. Phillips, R. Braun, W. Wang, J. Gumbart, E. Tajkhorshid, E. Villa, C. Chipot, R. D. Skeel and L. Kalé, *J Comput Chem*, 2008, **26**, 1781–1802.

9 D. MacKerell, A. D., Jr. Bashford, M. Bellott, J. D. Dunbrack, R. L. Jr. Evanseck, M. J. Field, S. Fischer, J. Gao, H. Guo, S. Ha, D. Joseph-McCarthy, L. Kuchnir, K. Kuczera, F. T. K. Lau, C. Mattos, S. Michnick, T. Ngo, D. T. Nguyen, B. Prodhom, W. E. Reiher, III., B. Roux, M. Schlenkrich, J. C. Smith, R. Stote, J. Straub, M. Watanabe, J. Wiorkiewicz-Kuczera, D. Yin and M. Karplus, *J Phys Chem B*, 1998, **102**, 3586–3616.

10 K. Huber and G. Herzberg, *Molecular spectra and molecular structure*, Van Nostrand Reinhold Company, New York, 1979.

11 U. Essmann, L. Perera, M. L. Berkowitz, T. Darden, H. Lee and L. G. Pedersen, *J Chem Phys*, 1995, **103**, 31–34.

12 J.-P. Ryckaert, G. Ciccotti and H. J. C. Berendsen, *J Comput Phys*, 1977, **23**, 337–341.

13 H. Grubmüller, H. Heller, A. Windemuth and K. Schulten, *Mol simulations*, 1991, **6**, 121–142.

14 G. J. Martyna, D. J. Tobias and M. L. Klein, *J Chem Phys*, 1994, **101**, 4177–4189.

15 S. E. Feller, Y. H. Zhang, R. W. Pastor and B. R. Brooks, *J Chem Phys*, 1995, **103**, 4613–4621.

16 W. Humphrey, A. Dalke and K. Schulten, *J Mol Graph*, 1996, **14**, 33–38.

17 D. A. Svistunenko, *Biochim Biophys Acta*, 2005, **1707**, 127–155.

18 L. Josimović, I. Janković and S. V. Jovanović, *Radiat Phys Chem*, 1993, **41**, 835–841.

19 G. Boguta and z A. Dancewic, *Int J Radiat Biol Relat Stud Phys Chem Med*, 1981, **39**, 163–174.

20 E. P. L. Hunter, M. F. Desrosiers and M. G. Simic, *Free Radic Biol Med*, 1989, **6**, 581–585.
21 M. R. Gunther, J. Andrew Peters and M. K. Sivaneri, *J Biol Chem*, 2002, **277**, 9160–9166.
22 A. Samuni and P. Neta, *J Phys Chem*, 1973, **77**, 1–7.
23 S. Carballal, B. Alvarez, L. Turell, H. Botti, B. A. Freeman and R. Radi, *Amino Acids*, 2007, **32**, 543–551.
24 J. Mönig, K. D. Asmus, L. G. Forni and R. L. Willson, *Int J Radiat Biol Relat Stud Phys Chem Med*, 1987, **52**, 589–602.
25 M. D. Sevilla, D. Becker and M. Yan, *J Radiat Biol*, 1990, **57**, 65–81.
26 M. D. Sevilla, M. Yan and D. Becker, *Biochem Biophys Res Commun*, 1988, **155**, 405– 410.
27 C. Schöneich, *Biochim Biophys Acta*, 2005, **1703**, 111–119.
28 C. Schöneich, *Arch Biochem Biophys*, 2002, **397**, 370–376.
29 Z. Ma, H. R. Williamson and V. L. Davidson, *Biochem J*, 2016, **473**, 1769–1775.